Vacancies on the Si(001) c(4*2) surface

1994 J. Phys.: Condens. Matter 6 9551

(http://iopscience.iop.org/0953-8984/6/45/006)

J. Phys.: Condens. Matter 6 (1994) 9551–9560. Printed in the UK

Vacancies on the Si(001) c(4 × 2) surface

K C Low, H S Lim and C K Ong

Department of Physics, National University of Singapore, Kent Ridge, Singapore 0511, Singapore

Received 17 May 1994, in final form 26 July 1994

Abstract. We have employed a parametrized tight-binding molecular-dynamics scheme in the study of the phenomenon of vacancies on the Si(001) c(4 × 2) surface. Simulated annealing is performed with a 'fictitious-Lagrangian' procedure to determine the optimal structures of a single and a dimer vacancy on this surface. A monovacancy is found to be less stable than a dimer vacancy, which agrees with experimental observations. We also show that there is a possible anisotropy in the surface migration of a dimer vacancy on the surface. The calculated activation energy for dimer-vacancy diffusion is 0.6 eV higher than that estimated experimentally at high temperatures.

1. Introduction

Interest in the Si(001) surface derives from its importance to device physics since many devices are grown on Si in the (001) orientation. Hence it is important to understand the structure of this surface and the defects that are likly to occur on it. Although much work, both theoretical and experimental, has been expended in the study of the electronic and structural properties of this surface, there has been relatively little work done to study the nature of intrinsic defects on this surface [1–4]. Recent scanning-tunnelling-microscopy (STM) experiments [1, 5, 6] consistently detect the presence of a large number of missing dimers. Thus, missing atoms seem to be a constant feature of this surface.

Analogous to vacancies on the surface is the presence of adatom(s). Possible anisotropy in the surface migration of adatoms on Si(001) surfaces has already been theoretically predicted with first-principles calculations [7], using the semi-empirical approach [8], as well as molecular-dynamics (MD) simulation [9] and Monte Carlo (MC) simulation [10] based on classical interatomic potentials. This phenomenon has been verified by STM experiments [11]. In the case of vacancies, it was observed recently in several ion-bombardment experiments on Si(001) surfaces [12] coupled with observations by STM that vacancies produced as a result of the ion bombardment are ordered into line defects perpendicular to the dimer rows upon annealing at elevated temperature. This suggests the existence of anisotropy in the surface migration of vacancies at high temperatures. Ultra-high-vacuum (UHV) reflection electron microscopy (REM) [13] has also determined that this phenomenon of vacancy diffusion on the Si(001) surface indeed has an anisotropic characteristic. In addition, several experiments using diffraction oscillations [14] and STM experiments [15] have established that the evolution of both metal and Si surfaces under low-energy (< 250 eV) ion bombardment is mediated by mobile surface vacancies created during sputtering. Specifically, mobile surface vacancies can nucleate monolayer-deep depressions or vacancy islands and can annihilate at step edges. Hence, vacancies on the Si(001) surface and their migration are very important phenomena.

0953-8984/94/459551+10$19.50

In this paper, we employ a semiempirical tight-binding (TB) MD scheme [4, 16] to study the presence of vacancies on Si(001) c(4 × 2) surfaces. This scheme is more efficient than that using local-density-approximation (LDA) calculations and more accurate than that using classical potentials. It is also better suited to study fairly large and complex Si systems for a reasonably long period of simulation. To show the reliability of this scheme in the study of vacancy on the surface, we have first calculated the formation energies of vacancies in the bulk using samples of different sizes with the supercell method. The c(4 × 2) surface consists of buckled dimers. We remove alternately the up and down atoms of a single dimer and relax the resultant structure by simulated annealing. The corresponding formation energies are calculated; we determine that the vacancy with the up atom is energetically favoured with respect to the down-atom vacancy. However, these two structures are unstable and a more stable structure is a dimer vacancy. We will show that the symmetry of the surface has an influence on the appearance of the dimer vacancy. We have also estimated the lower limit of the activation energy of self-diffusion of the dimer vacancy along and across the dimer rows.

2. The computational model

2.1. Tight-binding molecular dynamics

One of the central problems of theoretical solid-state physics is finding ways of calculating the forces acting between atoms in a solid. This is particularly important as the behaviour of near defects such as vacancies, dislocations and grain boundaries is affected by such forces. A correct description of these forces would thus enable an accurate prediction of mechanical and thermal properties of the materials. Moreover, knowledge of the forces acting upon each ion for an arbitrary atomic arrangement is required in the MD simulations of ionic trajectories. Whether the force expressions are difficult to obtain depends entirely on the complexity of the energy expressions. For simulation purposes, a compromise must be reached between simplicity and accuracy.

In the present work, we incorporate the MD techniques into the TB total-energy scheme for Si, following the prescription of Khan and Broughton (KB) [16]. This involves modifying the total-energy expression of Tomanek and Schluter (TS) [17] by appropriate smooth cut-off functions to permit MD simulations. This expression allows large deviations of the atoms from bulk equilibrium bond lengths and contains a Hubbard-like term for charging effects. We also follow their scheme of constructing a fictitious Lagrangian to simulate the physical trajectories of the nuclei while keeping the electrons close to their quantum ground state.

2.2. The total-energy calculation

In our simulation of the Si(001) surface, we use a slab of five layers of Si atoms with 32 atoms per layer for a total of 160 atoms. The top layer, in the positive z direction, forms a surface. Periodic boundary conditions are applied in the plane of the surface to simulate a surface extending to infinity in the x and y directions. In this simulation cell, the smallest separation between defects is six bond lengths. The interaction between defects is then expected to be small. In addition, a layer of H-like atoms is used to saturate the lowest layer of Si atoms. These 'H' atoms are meant to mimic Si atoms in the bulk and their parameters in the total-energy expression for the slab are chosen to simulate Si atoms.

During the simulations, the ions in the top four layers are allowed to move and interact with neighbouring atoms while the last two bottom layers (Si and the 'H' atoms in the

fifth and sixth layers, respectively) are kept fixed but are allowed to change their electronic structures as a result of interaction with neighbouring atoms. The total-energy expression used originates from that used by TS [17] and is similar to the one given by KB [16]. We also adopt the various TB parameter values suggested by TS and KB. Details of our algorithms can be found in [4]. The TB band-structure calculation is performed at the point $k = 0$ (Γ point) within the Brillouin zone (BZ). The Γ-point approximation is justified since the real-space computational cells we use are much larger than the primitive unit cell of Si. The larger real-space computational cell will yield a smaller BZ.

In our study of vacancy in the bulk, we use two cubes of 63 and 215 atoms respectively. Periodic boundary conditions are imposed in the x, y and z directions to simulate the bulk extending to infinity in the three directions. There are no 'H' atoms as in the study of the surface.

2.3. Molecular dynamics for the electrons and ions

In MD simulation, we start with approximate atomic coordinates and atomic velocities. We then proceed to solve the electronic-structure problem for these atomic configurations. In our TB scheme, this is equivalent to diagonalizing the Hamiltonian matrix. The Born–Oppenheimer (BO) approximation, which states that the total energy could be kept at a minimum at all times with respect to the electronic coordinates, subject to the orthonormality constraints of the wave functions, is assumed in our simulation. This minimization is frequently referred to as quenching the electrons to the BO surface.

After each quench, the trajectories of both the ionic and electronic coordinates are updated simultaneously with the Verlet algorithm. This is repeated for 100 time steps after which the electrons are quenched to the BO surface again and the procedure repeated. During the 100 steps, a 'Shake' algorithm [19] is used to impose the orthonormality constraints in the updating of the electronic coordinates.

3. Results and discussion

In each of our samples, we heat up the system and then cool it slowly to $T = 0$ K by appropriately scaling the velocities of the atoms. This annealing treatment is repeated a few more times to make sure that the resulting system is at least in a local minimum.

The formation of a vacancy requires the energy for (i) the removal of an atom from the interior of a crystal ($E_v[N-1] - E[N]$) and (ii) its replacement at the kink site on the surface ($E_{bulk}[N]/N$). The formation energy (E_f) of a vacancy can then be written as

$$E_f = E_v[N-1] - E[N] + E_{bulk}[N]/N \tag{1}$$

where $E_v[N-1]$ is the total energy of the defect system with $N-1$ atoms, $E[N]$ is the total energy of the perfect system (i.e., without defects) of N atoms, and $E_{bulk}[N]$ is the energy of N Si atoms in the bulk phase.

3.1. Bulk vacancy

For the problem of a monovacancy in crystalline Si, the absence of an Si atom produces four dangling bonds on the four nearest atoms around the vacancy. These nearest atoms are now threefold coordinated, with a geometry similar to the top-layer atoms on the Si(111) surface. By analogy with the Si(111) surface, we would expect the nearest atoms around the

bulk vacancy to relax away from the void due to the strengthening of their back bonds, as predicted by early LDA calculation [19] and classical interatomic potential [21]. However, this idea has been challenged by recent LDA calculations [22], which have predicted that the atoms around the defect relax toward it, instead of away from it. Hence, the vacancy structure is a challenge for this scheme.

Since monovacancy in Si has been studied extensively, we aim to use it as an initial test of our method. We therefore report our results to compare with those obtained from LDA [22], classical potential [25] and other similar TBMD schemes [24].

We use a large unit cell (LUC) of 64 atoms and 216 atoms with periodic conditions applied in all three directions. The LUC has to be large enough to minimize the defect–defect interactions. The interaction arises through the strain field created by the defect. We have calculated the average displacements of atoms around the monovacancy from our 216-atom LUC studies and present them in table 1. The average displacements around the void decreases rapidly as the distance from the void increases. At the distance of four bond lengths away from the void, which is equal to 9.4 Å, the distortion is only 0.01 Å. For the 216-atom periodic LUC, the distance between voids is 16.35 Å and therefore suitable for the bulk vacancy study. For the case of the 64-atom LUC, which has dimensions of 10.9 Å, there are some defect–defect interactions due to propagation of the strain field across the cell boundary. The calculated formation energies from our present study, together with results from the LDA, classical interatomic potential, other TBMD schemes and experimental results are reported in table 2. In general, the LDA uses a smaller LUC and risks including defect–defect interactions or defect–surface interactions, while the classical potential method uses a much larger LUC but neglects the details of electronic effects. On the whole, all the results quoted in table 2 give a reasonable account of the experimental data. We also analysed the details of displacements of the four nearest neighbours of the monovacancy and present them in table 3. The configuration of the monovacancy and its neighbours is illustrated in figure 1. After the relaxation of the nearest atoms, the tetrahedral symmetry around the vacancy is broken. Atom a pairs with atom c and atom g with h. In addition to the pairing movement along the ⟨110⟩ direction, all the four nearest atoms are relaxed toward the voids. Our result is in general agreement with the conclusion of Watkins drawn from his electron-paramagnetic-resonance experiments [23]. Antonelli and Bernholc [22] obtained the inward radial displacements of the nearest neighbours to be 0.07 Å, which is an order of magnitude smaller than the results obtained here. Glassford *et al* [25] obtained an inward displacement of 0.4 Å from their classical interatomic potential, which is similar to our results. However, experimental information on the details of displacement is still lacking.

Table 1. The average lattice displacement of atoms around the monovacancy as a function of distance from the monovacancy.

No of bond-length distances away from the void	Average displacement (Å)
1	0.513
2	0.078
3	0.017
4	0.011

3.2. Monovacancy on the reconstructed surface

We first calculate the formation energy and equilibrium configuration of a monovacancy case by alternately removing an up- and a down atom of a dimer from a relaxed Si(001)

Table 2. Si defect formation energy of the bulk predicted with other methods, *ab initio*, TB or classical. Also included is the experimental result obtained by a positron-annihilation experiment in Si. The numbers in brackets are the numbers of atoms in the computational LUC.

References	Formation energy (eV)
Ab inito calculations, LDA [20, 22, 29]	3.6–5.0 (< 32 atoms)
TB calculations [24]	3.67 (64 atoms)
	3.96 (216 atoms)
	4.12 (512 atoms)
Classical potentials [21]	3.8
[25]	4.7
Experimental result [30]	3.6 ± 0.2
Present calculation	3.94 (64 atoms)
	3.59 (216 atoms)

Table 3. The detailed displacements of nearest atoms (see figure 1) around the monovacancy.

	Displacements (Å)		
Atom	Δx	Δy	Δz
a	−0.255	+0.239	+0.283
c	+0.223	+0.270	+0.280
g	+0.333	+0.349	−0.364
h	−0.312	−0.332	−0.311

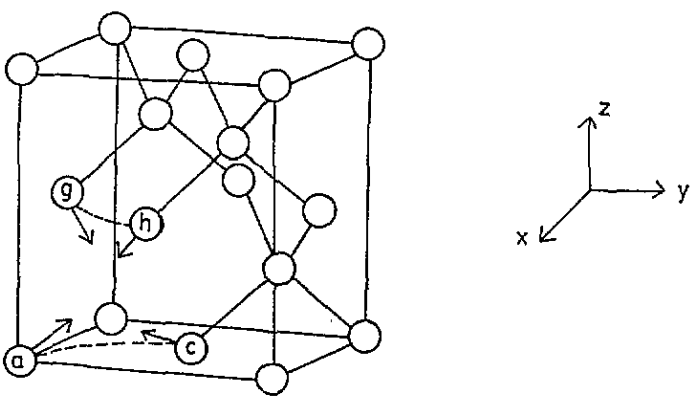

Figure 1. The atomic geometry of a vacancy in crystalline Si. The arrows on atoms a, c, g and h indicate the distortions of the lattice around the vacancy. The dotted lines connect the pairing atoms. Note that the relaxation of the atoms nearest to the vacancy is towards the vacancy.

c(4 × 2) surface. The metastable configurations for the up-atom vacancy and the down-atom vacancy are illustrated in figure 2. The formation energies have been calculated and are tabulated in table 4. Thus the formation of the up-atom vacancy is energetically favoured with respect to the down-atom vacancy.

Table 4. Vacancies on the Si(001) c(4 × 2) surface and the corresponding formation energy.

Atom removed	Formation energy (eV)
Up atom	0.76
Down atom	0.95

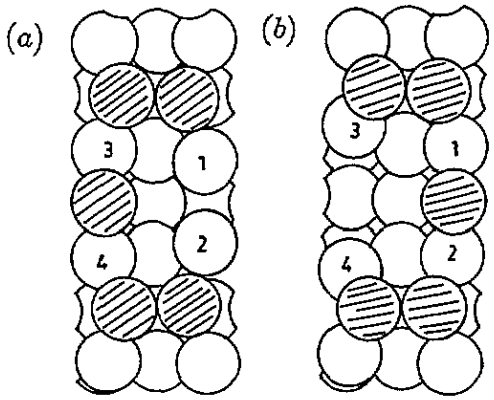

Figure 2. The metastable configuration of (*a*) the up-atom and (*b*) the down-atom vacancy on the Si(001) c(4 × 2) surface. Surce Si atoms are shown as shaded circles and second- and third-layer atoms are shown as open circles.

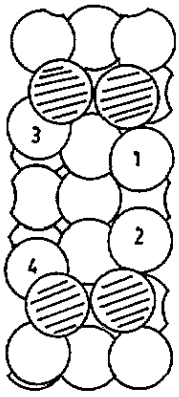

Figure 3. The optimal configuration of a divacancy on the Si(001) c(4×2) surface. Surface Si atoms are shown as shaded circles and second- and third-layer atoms are shown as open circles.

In the metastable configuration of the up-atom vacancy, the two exposed second-layer atoms (atoms 1 and 2 of figure 2(*a*)) are directed to form a weak bond. In the case of the down-atom vacancy, the exposed second-layer atoms (atoms 3 and 4 of figure 2(*b*)) are driven away from the vacancy due to the need to relax their back bonds. Therefore it is not surprising that the up-atom vacancy is energetically more stable than the down vacancy because the formation of the weak bond reduces the high energy associated with the remaining dangling bonds.

A common feature of the two metastable configurations of the different vacancies is that the remaining atom of the 'defect dimer' moves (in both cases) to form a plane with the two nearest second-layer atoms, which is perpendicular to the surface. These remaining atoms are unstable as we will see in the next section. Furthermore, STM does not observe monovacancies on the Si(001) surface and therefore the monovacancy must have a short life. However, the mechanism of the disappearance of the remaining atom of the 'defect dimer' is not clear. Zhang and Metiu [26] use the kinetic approach to argue that the remaining atom of the 'defect dimer' will be repelled rapidly to the easy-diffusion channel along the dimer row and also possibly by the arrival of the adatom at the vacancy site.

3.3. Divacancy on the reconstructed surface

We proceed next to remove the remaining atom of the 'defect dimer' of the two metastable configurations shown in figure 2 to form a divacancy. The two relaxed structures are similar and hence only one is shown in figure 3. The formation energies of a divacancy from an up or a down vacancy have been calculated and are tabulated in table 5. In both cases, the formation energy is negative! Hence, the monovacancy on the Si(001) surface is energetically unstable and will expel the remaining atom of the 'defect dimer' to form a

divacancy. This is in agreement with STM experiments [5] where many defects are observed, the smallest defect being a divacancy.

Table 5. Divacancies on the Si(001) c(4 × 2) surface and the corresponding formation energy from the up vacancy and the down vacancy.

Initial vacancy	Formation energy (eV)
Up vacancy	−0.15
Down vacancy	−0.35

From the stable configuration of the divacancy in figure 4, among the four exposed second-layer atoms, two move toward each other to form a weak bond while the other pair move away from each other, driven by the need to relax their back bonds. We note that the adjacent dimers beside the divacancy, in the neighbouring dimer rows, are buckled in the opposite sense. The dimer beside the weak bond of the two exposed second-layer atoms is buckled with the up atom nearest to the defect. In contrast, the dimer beside the separation of the two exposed second-layer atoms is buckled with the down atom nearest to the divacancy. This is consistent with the result of Lim *et al* [4] in their study of the dynamical behaviour of dimers and divacancies on an Si(001) surface. Hence we note that the particular geometry of a divacancy on the Si(001) c(4 × 2) surface is the result of the constraints imposed by the symmetry of the surface. Wang *et al* [3], using LDA calculation, determine the formation energy of a divacancy on an Si(001) (2 × 1) surface to be 0.22 eV/dimer for the energetically most stable structure, where the four exposed second-layer atoms approach each other to form two weak bonds. We calculate the formation energy of a divacancy to be ∼ 0.6 eV, which is the sum of corresponding values from tables 4 and 5. This is closer to the value of 0.64 eV/dimer calculated by Wang *et al* [3] for the metastable structure where no weak bonds are formed due to the strengthening of the back bonds of the exposed second-layer atoms.

We have also estimated the migration energy for self-diffusion of a divacancy along and across the dimer row. A realistic simulation would be one where a long simulation time is used, together with an elevated temperature and proper constant-pressure treatment imposed on the boundary conditions, and the actual migration observed. However, this will take much computational effort and expensive computational time. Here, we have instead calculated the fully relaxed mid-point configuration of the divacancy diffusion path along and across the dimer rows. The mid-point configurations along the dimer rows are illustrated in figure 4(*a*) and (*b*). For diffusion across the dimer rows, i.e. perpendicular to the dimer rows, the mid-point configurations are those in figure 4(*c*) and 4(*d*). We can then at least estimate the lower limit of the activation energy of diffusion.

In all the simulations to determine the fully relaxed mid-point configurations, the x and y coordinates of the atoms of the dimer that is 'moved' (the shaded circles in the figures) are fixed while the z coordinates are allowed to vary. The rest of the atoms of the system, except the two 'frozen' layers, are allowed to relax to their minimum configurations. The calculated migration energies are tabulated in table 6.

From the result for the migration energies, we note that the mid-point configuration of figure 4(*c*) appears to be the lowest activation barrier for a divacancy self-diffusion. However, there is a potential barrier of 2.61 eV that a divacancy must overcome to reach this mid-point configuration, as shown in figure 4(*d*). Comparing with the mid-point configuration of figure 4(*b*), our calculation confirms that there is an anisotropy in surface vacancy diffusion as observed in experiments [12, 13]. Our results show that surface

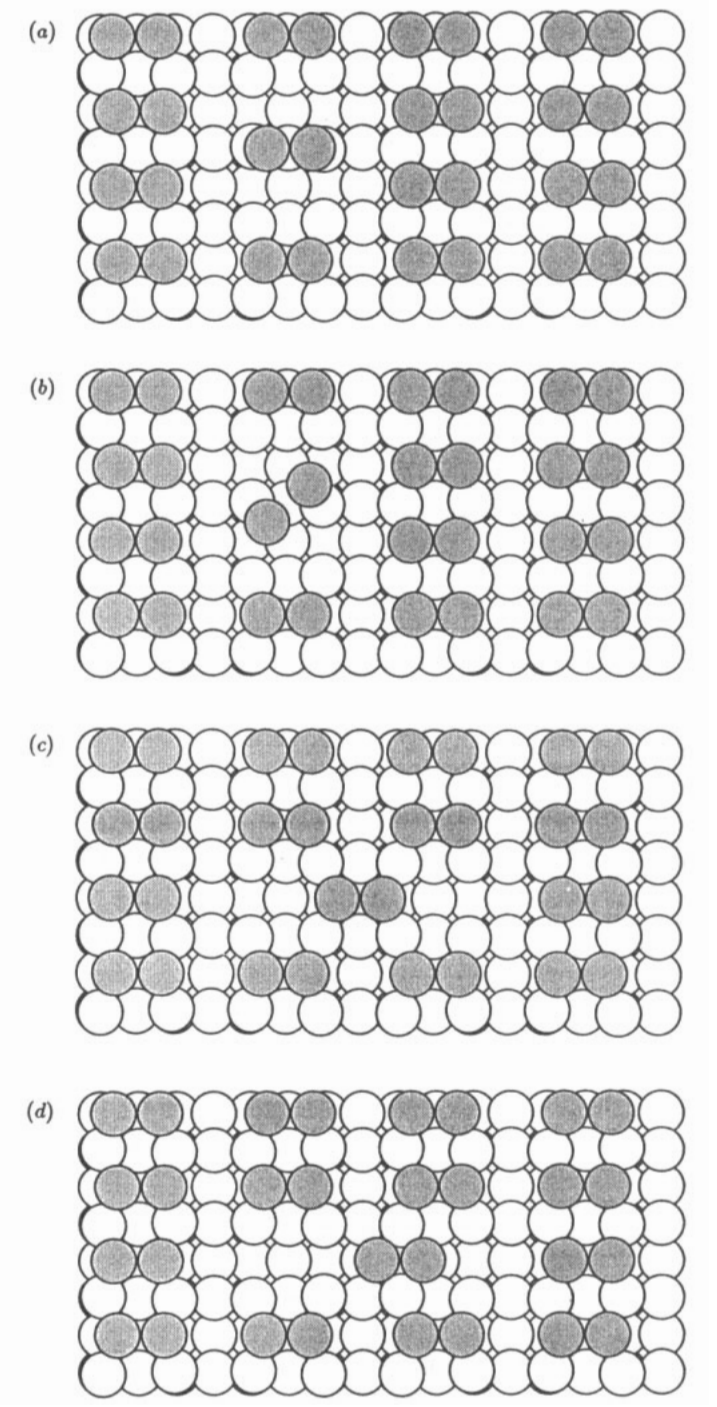

Figure 4. Several mid-point configurations for surface migration of a divacancy along and across dimer rows. (*a*) A configuration for self-diffusion of the divacancy along the dimer row. (*b*) An alternative configuration for self-diffusion of the divacancy along the dimer row. (*c*) A configuration for self-diffusion of the divacancy across the dimer row, i.e., in the direction perpendicular to the dimer rows. (*d*) The dimer moves half the distance to the mid-point configuration for self-diffusion of the divacancy across the dimer row.

Table 6. Migration energies for the various saddle-point configurations.

Mid-point of diffusion path	Migration energies (eV)
Figure 4(*a*)	4.31
Figure 4(*b*)	2.31
Figure 4(*c*)	0.42
Figure 4(*d*)	2.61

vacancy diffusion is easier along the dimer rows rather than across it. The migration energy of 2.31 eV is large compared with the 0.4 eV (for bulk-vacancy migration) calculated by Watkins [23] but is reasonable compared with experimental observations. In a low-energy ion bombardment [12], Feil *et al* observed by STM that the vacancies formed as a result of the bombardment are stable at room temperature. On annealing at 600 °C for 2 min, the random defects appeared to become ordered into line defects perpendicular to the dimer rows. Thus, we deduce that defects most likely diffuse along their respective dimer rows to form a line of defects perpendicular to the dimer rows. In addition the annealing temperature of 600 °C suggests that the vacancies need sufficiently large kinetic energies to overcome the migration barriers. Therefore, our result is similar to experimental observation.

In addition, from the migration energies, we observe that a divacancy diffusing along the dimer row (or a dimer diffusing along a dimer row) does not break the two bonds of the neighbouring dimer simultaneously, as in figure 4(*a*), but rather one bond is broken at a time as in figure 4(*b*). This is similar to the process that Wang *et al* [3] propose for a divacancy diffusing along its dimer row. Wang *et al* [3] estimate the energy-barrier height for the diffusion of a divacancy along a dimer row on a (2 × 1) surface to be about 2.4 eV, which is close to our calculation of 2.31 eV. Recent STM experiments by Kitamura and co-workers [27] determine an activation energy of 1.7 ± 0.4 eV. Our result is different from the experimental data partly because our surface is (4 × 2) and the calculation is done at $T = 0$. However, the experiment [27] was performed at 500 K where the dimers are oscillating to give an appearance of symmetric dimers [5, 28]. Another possible reason for the deviation of the activation energy from the experimental estimation is the fact that the diffusion mechanisms involve only surface atoms in our calculations. Recently, Zhang and co-workers [31] have suggested a different mechanism of diffusion, via a wavelike concerted motion involving atoms from the top and second layers, which yields a lower activation energy. Unfortunately, it is still not possible to trace the trajectories of a divacancy in a realistic simulation time with current computer technology.

4. Conclusion

In conclusion, we have studied the phenomenon of vacancy on the Si(001) c(4 × 2) surface. We first established the reliability of this semiempirical tight-binding molecular-dynamics scheme by determining the formation energy of a bulk vacancy. We have also shown that monovacancies are unstable on this surface and the smallest type of vacancy is the divacancy, as observed by STM experiments. From the optimal structure of this divacancy, we determine that the appearance of the defect is constrained by the symmetry of the surface. We have also determined the existence of an anisotropy in the surface migration of the divacancy, which is observed by various low-energy ion-bombardment experiments coupled with observations by STM. The estimated activation energy of divacancy migration agrees with those from LDA calculation [3] but is higher than the experimental value by 0.6 eV.

References

[1] Hamers R J and Kohler U K 1989 *J. Vac. Sci. Technol.* A 7 2854
[2] Roberts N and Needs R J 1989 *J. Phys.: Condens. Matter* **1** 3139; 1990 *Surf. Sci.* **236** 112
Ihara S, Ho S L, Uda T and Hirao M 1990 *Phys. Rev. Lett.* **64** 1909
[3] Wang J, Arias T A and Joannopoulos J D 1993 *Phys. Rev.* B **47** 10497
[4] Lim H S, Low K C and Ong C K 1993 *Phys. Rev.* B **48** 1595
[5] Tromp R M, Hamers R J and Demuth J E 1985 *Phys. Rev. Lett.* **55** 1303
Hamers R J, Tromp R M and Demuth J E 1986 *Phys. Rev.* B **34** 5343
[6] Alerhand O L, Berker N A, Joannopoulos J D, Vanderbilt D, Hamers R J and Demuth J E 1990 *Phys. Rev. Lett.* **64** 2406
[7] Miyazaki T, Hiramoto H and Okazaki M 1990 *Japan. J. Appl. Phys.* **29** L1165
Brocks G, Kelly P J and Car R 1991 *Phys. Rev. Lett.* **66** 1729
[8] Ong C K 1993 *J. Phys. Chem. Solids* **54** 183
[9] Srivastava D and Garrison B J 1991 *J. Chem. Phys.* **95** 6885
[10] Toh C P and Ong C K 1992 *Phys. Rev.* B **45** 11120
[11] Mo Y-W, Swartzentruber B S, Kariotis R, Webb M B and Lagally M G 1989 *Phys. Rev. Lett.* **63** 2393
Mo Y-W and Lagally M G 1991 *Surf. Sci.* **248** 313
[12] Bedrossian P and Klitsner T 1992 *Phys. Rev. Lett.* **68** 646
Feil H, Zandvliet H J W, Tsai M H, Dow J D and Tsong I S T 1992 *Phys. Rev. Lett.* **69** 3076
Zandvliet H J W, Elswijk H B, van Loenen E J and Tsong I S T 1992 *Phys. Rev.* B **46** 7581
[13] Kahata H and Yagi K 1989 *Japan. J. Appl. Phys.* **28** L1042
[14] Poelsema B, Verheij L and Comsa G 1984 *Phys. Rev. Lett.* **53** 2500
Bedrossian P, Houston J E, Chason E, Tsao J Y and Picraux S T 1991 *Phys. Rev. Lett.* **67** 124
[15] Michely T, Besocke K and Comsa G 1990 *Surf. Sci. Lett.* **230** L135
Bedrossian P and Klitsner T 1991 *Phys. Rev.* B **44** 13783
[16] Khan F S and Broughton J Q 1989 *Phys. Rev.* B **39** 3688
[17] Tomanek D and Schluter M A 1986 *Phys. Rev. Lett.* **56** 1055; 1987 *Phys. Rev.* B **36** 1208
[18] Alerhand O L and Mele E J 1987 *Phys. Rev.* B **35** 5533
[19] Ryckaert J P, Ciccotti G and Berendsen H J C 1977 *J. Comput. Phys.* **23** 327
[20] Baraff G A, Kane O and Schluter M 1980 *Phys. Rev.* B **21** 5662
[21] Biswas R and Hamann D 1985 *Phys. Rev. Lett.* **55** 2001; 1987 *Phys. Rev.* B **36** 6434
[22] Antonelli A and Bernholc J 1989 *Phys. Rev.* B **40** 10643
[23] Watkins G D 1986 *Deep Centers in Semiconductors—a State-of-the-Art Approach* ed S T Pantelides (New York: Gordon and Breach) p 147
[24] Wang C Z, Chan C T and Ho K M 1991 *Phys. Rev. Lett.* **66** 189
[25] Glassford K M, Chelikowsky J R and Philips J C 1991 *Phys. Rev.* B **43** 14557
[26] Zhang Z and Meitu H 1993 *Phys. Rev.* B **48** 8166
[27] Kitamura N, Lagally M G and Webb M B 1993 *Phys. Rev. Lett.* **71** 2082
[28] Wolkow R A 1992 *Phys. Rev. Lett.* **68** 2636
[29] Car R, Kelly P J, Oshiyama A and Pantelides S T 1984 *Phys. Rev. Lett.* **52** 1814; 1985 *Phys. Rev. Lett.* **54** 360
Bar-Ham Y and Joannopoulos J D 1984 *Phys. Rev. Lett.* **52** 1129; 1984 *Phys. Rev.* B **30** 1844
[30] Varotsos P, Eftaxias K and Hadjicontis V 1988 *Phys. Rev.* B **38** 6328
[31] Zhang Z, Chen H, Bolding B C and Lagally M G 1993 *Phys. Rev. Lett.* **71** 3677